Important Notice to Authors

Attached is a PDF proof of your forthcoming article in PRB. Your article has 11 pages and the Accession Code is **BF12747**.

Please note that as part of the production process, APS converts all articles, regardless of their original source, into standardized XML that in turn is used to create the PDF and online versions of the article as well as to populate third-party systems such as Portico, CrossRef, and Web of Science. We share our authors' high expectations for the fidelity of the conversion into XML and for the accuracy and appearance of the final, formatted PDF. This process works exceptionally well for the vast majority of articles; however, please check carefully all key elements of your PDF proof, particularly any equations or tables.

Figures submitted electronically as separate PostScript files containing color appear in color in the online journal. However, all figures will appear as grayscale images in the print journal unless the color figure charges have been paid in advance, in accordance with our policy for color in print (http://journals.aps.org/authors/color-figures-print). For figures that will be color online but grayscale in print, please ensure that the text and captions clearly describe the figures to readers who view the article only in grayscale.

No further publication processing will occur until we receive your response to this proof.

Specific Questions and Comments to Address for This Paper

1 The .eps file for Fig. 3 does not match the ones in the PDF you supplied. Please confirm that the correct figure was used.
2 We have deleted text of part label in Fig. 9. Please check.
3 Please check Ref. [8] for accuracy.
4 Ref. [9] volume and page number added. Please check.
5 Please provide publisher location in Refs. [12,31].
6 Please remove duplicate entry (i.e., Refs. [21] and [37]) from the reference list and renumber all subsequent reference citations in both the text and in the reference list.
7 Please complete Ref. [32].
8 Please update arXiv in Ref. [34], if published.
FQ: This funding provider could not be uniquely identified during our search of the FundRef registry. Please check information and amend if incomplete or incorrect.
Q: This reference could not be uniquely identified due to incomplete information or improper format. Please check all information and amend if applicable.

Titles in References: The editors now encourage insertion of article titles in references to journal articles and e-prints. This format is optional, but if chosen, authors should provide titles for *all* eligible references. If article titles remain missing from eligible references, the production team will remove the existing titles at final proof stage.

FundRef: Information about an article's funding sources is now submitted to CrossRef to help you comply with current or future funding agency mandates. Please ensure that your acknowledgments include all sources of funding for your article following any requirements of your funding sources. CrossRef's FundRef registry (http://www.crossref.org/fundref/) is the definitive registry of funding agencies. Please carefully check the following funder information we have already extracted from your article and ensure its accuracy and completeness:

NSF (USA), CMMI-0953984, DMR-0805293, DMR-DMR-0844082
National Science Foundation (USA), ACI-1053575
Deutsche Forschungsgemeinschaft (Germany), SPP 1599
CONACYT (Mexico), 152153
NSF (USA), DMREF-NSF 1434897
American Chemical Society Petroleum Research Fund (USA), 54075-ND10

Other Items to Check

- Please note that the original manuscript has been converted to XML prior to the creation of the PDF proof, as described above. Please carefully check all key elements of the paper, particularly the equations and tabular data.
- Please check PACS numbers. More information on PACS numbers is available online at http://journals.aps.org/PACS/.
- Title: Please check; be mindful that the title may have been changed during the peer review process.
- Author list: Please make sure all authors are presented, in the appropriate order, and that all names are spelled correctly.
- Please make sure you have inserted a byline footnote containing the email address for the corresponding author, if desired. Please note that this is not inserted automatically by this journal.
- Affiliations: Please check to be sure the institution names are spelled correctly and attributed to the appropriate author(s).
- Receipt date: Please confirm accuracy.
- Acknowledgments: Please be sure to appropriately acknowledge all funding sources.

- Hyphenation: Please note hyphens may have been inserted in word pairs that function as adjectives when they occur before a noun, as in "x-ray diffraction," "4-mm-long gas cell," and "*R*-matrix theory." However, hyphens are deleted from word pairs when they are not used as adjectives before nouns, as in "emission by x rays," "was 4 mm in length," and "the *R* matrix is tested."

  Note also that Physical Review follows U.S. English guidelines in that hyphens are not used after prefixes or before suffixes: superresolution, quasiequilibrium, nanoprecipitates, resonancelike, clockwise.
- Please check that your figures are accurate and sized properly. Make sure all labeling is sufficiently legible. Figure quality in this proof is representative of the quality to be used in the online journal. To achieve manageable file size for online delivery, some compression and downsampling of figures may have occurred. Fine details may have become somewhat fuzzy, especially in color figures. The print journal uses files of higher resolution and therefore details may be sharper in print. Figures to be published in color online will appear in color on these proofs if viewed on a color monitor or printed on a color printer.
- Please check to ensure that titles are given as appropriate.
- ***Overall, please proofread the entire article very carefully.***

Ways to Respond

- ***Web:*** If you accessed this proof online, follow the instructions on the web page to submit corrections.
- ***Email:*** Send corrections to prbproofs@aptaracorp.com
  Subject: **BF12747** proof corrections
- ***Fax:*** Return this proof with corrections to +1.703.791.1217. Write **Attention:** PRB Project Manager and the Article ID, **BF12747**, on the proof copy unless it is already printed on your proof printout.
- ***Mail:*** Return this proof with corrections to **Attention:** PRB Project Manager, Physical Review B, c/o Aptara, 3110 Fairview Park Drive, Suite #900, Falls Church, VA 22042-4534, USA.

PHYSICAL REVIEW B **00**, 004100 (2015)

Stability analysis of the martensitic phase transformation in Co_2NiGa Heusler alloy

Anjana Talapatra,[1,*] Raymundo Arróyave,[1,2] Peter Entel,[3] I. Valencia-Jaime,[4,5] and Aldo H. Romero[5]

[1]*Department of Mechanical Engineering, Texas A&M University, College Station, Texas 77843, USA*

[2]*Department of Materials Science & Engineering, Texas A&M University, College Station, Texas 77843, USA*

[3]*Faculty of Physics and CENIDE, University of Duisburg-Essen, 47048 Duisburg, Germany*

[4]*CINVESTAV-Querétaro, Libramiento Norponiente No. 2000, Real de Juriquilla, 76230 Querétaro, México*

[5]*Department of Physics, West Virginia University, Morgantown, West Virginia 26506, USA*

(Received 3 June 2015; revised manuscript received 30 July 2015; published xxxxxx)

Phase competition and the subsequent phase selection are important characteristics of alloy systems exhibiting numerous states of distinct symmetry but comparable energy. The stoichiometric Co_2NiGa Heusler alloy exhibits a martensitic transformation with concomitant reduction in symmetry from an austenitic $L2_1$ phase (cubic) to a martensitic $L1_0$ phase (tetragonal). A structural search was carried out for this alloy and it showed the existence of a number of structures with monoclinic and orthorhombic symmetry with ground state energies comparable to and even less than that of the $L1_0$ structure, usually reported as the ground state at low temperatures. We describe these structures and focus in particular on the structural transition path from the $L2_1$ to tetragonal and orthorhombic structures for this material. Calculations were carried out to study the Bain ($L2_1$-$L1_0$) and Burgers ($L2_1$-hcp) transformations. The barrierless Burgers path yielded a stable martensitic phase with orthorhombic symmetry (O) with energy much lower—beyond the expected uncertainty of the calculation methods—than the known tetragonal $L1_0$ martensitic structure. This low-energy structure (O) has yet to be observed experimentally and it is thus of scientific interest to discern the cause for the apparent discrepancy between experiments and calculations. It is postulated that the Co_2NiGa Heusler system exhibits a classic case of the phase selection problem: although the unexpected O phase may be relatively more stable than the $L1_0$ phase, the energy barrier for the ($L2_1$-O) transformation may be much higher than the barrier to the ($L2_1$-$L1_0$) transformation. To validate this hypothesis, the stability of this structure was investigated by considering the contributions of elastic and vibrational effects, configurational disorder, magnetic disorder, and atomic disorder. The calculations simulating the effect of magnetic disorder/high temperature as well as the atomic disorder simulations showed that the transformation from $L2_1$ to $L1_0$ is favored over the Burgers path at high temperatures (large magnetic disorder). These conditions are prevalent upon cooling the material from high temperatures (the usual synthesis route), and this provides a plausible explanation of why $L1_0$ and not the O phase is observed. Other ground states (not observed in experiments but predicted through calculations) are ruled out in terms of symmetry relations as well as through considerations of elastic barriers to their nucleation.

DOI: 10.1103/PhysRevB.00.004100 PACS number(s): 64.60.−i

I. INTRODUCTION

Over the last few decades, experimental and theoretical research into shape memory alloys (SMAs) has gained momentum due to the need for high-temperature multifunctional materials. Current applications of SMAs are restricted to below 100 °C for NiTi-based and Cu-based alloys which have transformation temperatures in that range. To be able to realize the advantages offered by these multifunctional materials in the automotive, aerospace, and heavy-machinery industries, there is a requirement for SMAs with much higher transformation temperatures. CoNiGa is one such promising SMA which is the object of much interest due to its potential as a magnetic SMA with a thermoelastic transition in the ferromagnetic state [1]. Cobalt has a large magnetic moment which ensures a high Curie temperature. The CoNiGa alloy is sufficiently ductile, exhibits the shape memory effect (SME), and has excellent superelastic properties [2]. Additionally, it shows martensitic start (M_s) temperatures up to 250 °C [3]. The CoNiGa alloy with a stoichiometric Heusler-type composition (Co_2NiGa) is a primary candidate for applications requiring ferromagnetic shape memory alloys [4–7].

Heusler alloys may be defined as ternary intermetallic compounds with a stoichiometric composition X_2YZ, with the $L2_1$ crystal symmetry. The $L2_1$ unit cell belongs to the space group $Fm\bar{3}m$ and the whole crystal shows only tetrahedral symmetry. X and Y are transition metals while Z is usually a covalently bonding group III-V element. The Heusler structure is bcc-like as it can be formed from the ordered combination of two binary B2 compounds XY and XZ with CsCl structure [8]. Austenitic Co_2NiGa exhibits the Heusler $L2_1$ structure (space group $Fm\bar{3}m$) with two interpenetrating binary B2 compounds CoNi and CoGa with a CsCl structure. The related inverse Heusler structure (CoNi)CoGa can be described as one in which the Co sublattice is occupied by the Ni atom, while the displaced Co atoms sit on the Ni sites. DFT calculations have shown that the inverse Heusler structure competes with the conventional Heusler structure in some cases [9].

In the Co_2NiGa system, there is a martensitic transformation from the ordered cubic $L2_1$ to the nonmodulated tetragonal $L1_0$ (AuCu, space group $P4/mmm$, 123) phase. Modulated martensites which are seen in Ni(Mn,Fe)Ga Heusler alloys have not been observed in the CoNiGa system [10,11]. The $L2_1$ to $L1_0$ transformation can be described as

*anjanatalapatra@tamu.edu

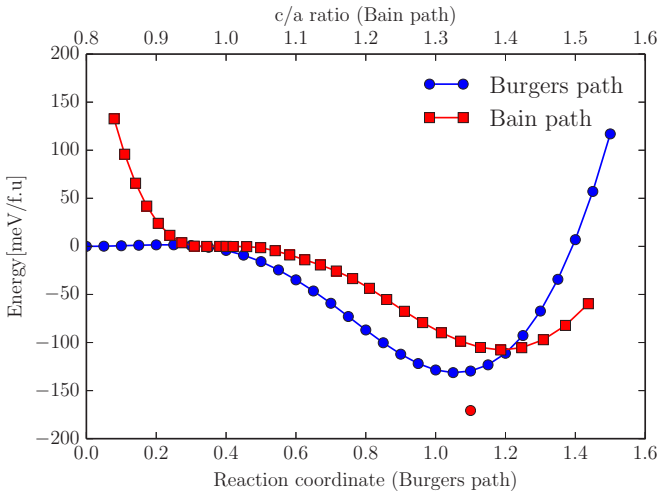

FIG. 1. (Color online) Energy profile comparison for Bain and single-parameter Burger paths in Co_2NiGa. The minimum along the Burgers path occurs at approximately $\delta = 1.1$ (O structure). The single data point in the figure corresponds to the completely relaxed minimum-energy structure.

a tetragonal distortion of the cubic austenitic phase. If one assumes that the transformation occurs with minimal volume change, then it can be described through a Bain path, which essentially transforms a bcc structure into a fcc variant as the c/a ratio of the lattice goes from 1 to $\sqrt{2}$. The Bain path shown in Fig. 1 (red curves) illustrates the transformation. In the figure, $c/a = 1$ corresponds to the $L2_1$ phase, while the minimum at $c/a = \sqrt{2}$ corresponds to the low-symmetry, low-energy martensite $L1_0$ with structural symmetry.

Along with the Bain mechanism, the body centered cubic (bcc)–hexagonal close packed (hcp) transformation is the most commonly observed reconstructive phase transformation in simple crystals. It is found in about 20 elements [12]. The mechanism used to describe this transformation is the Burgers path [13], first proposed for the β-α transformation in Zr. When applied to the CoNiGa system, surprisingly, the Burgers path is seen to be a barrierless transformation that reaches a minimum value at distortions resulting from shuffles and shears. This minimum corresponds to a low-energy martensitic structure with orthorhombic symmetry (space group 59), referred to as the O structure henceforth which is more stable (has a lower energy) than the conventional martensitic $L1_0$ structure. The O phase has yet to be reported in the literature and its absence in experiments cannot be merely explained away using kinetic barrier arguments as the transformation clearly can go forward in a monotonic way, at least under ground state—i.e., low temperature—conditions.

In an effort to explain this unprecedented O phase, an extensive investigation was carried out to provide insight into the phenomenon by exploring the energy landscape around the cubic Co_2NiGa composition. A structural search by using the minima hopping method [14] was carried out to explore the energy landscape surrounding the conventional martensitic $L1_0$ structure. These calculations predicted a number of structures with monoclinic, tetragonal, and orthorhombic symmetries with energies much lower than the $L1_0$ structure as well as the O phase, with energy differences much larger than typical computational errors within the chosen approximations. Various high-throughput databases such as the Materials Project [15], the Open Quantum Materials Database (OQMD) [16], and Automatic Flow for Materials Discovery (AFLOW) [17] did not yield any of the structures predicted by the minima hopping method (MHM) or the Burgers calculations. This may be attributed to the lesser number of known structures for ternary phases, making predictions based on data mining very difficult beyond binary systems or that those methods have been not used in particular for this type of compound.

Even with the extensive energy landscape exploration, the question as to why the Co-Ni-Ga system undergoes a martensitic transformation to the $L1_0$ phase while other lower energy structures, specifically the O phase which may be accessed via the Burgers path, exist still remains to be answered. The question may be addressed in either one of three ways: (i) DFT within a set of given approximations is inadequate to capture the energetics of the transformations in the Co-Ni-Ga system; (ii) experiments have so far been unable to isolate the true martensitic ground state of the system; (iii) the problem may be resolved by invoking phase competition/phase selection at elevated temperatures as the system cools down from a cubic austenitic state.

In addition to the structural search results, we also present total energy calculations for the Burgers transformation and Bain paths in the conventional Heusler and inverse Heusler Co_2NiGa alloys. It is postulated that the isolation of a low-energy martensitic phase which is more stable than the $L1_0$ martensite via *ab initio* calculations may be attributed to a classic case of the phase selection conundrum, wherein the Co_2NiGa $L2_1$ phase preferentially transforms to the $L1_0$ martensitic phase in spite of other possible structures which are inaccessible even though their energy is lower. Elastic and phonon calculations were carried out with the intention of isolating any instabilities due to vibrational or elastic effects. Finally, the Bain and Burgers paths were recalculated taking into consideration the effect of configurational, magnetic, and atomic disorder. This analysis indicates that there is probably a good explanation of why we do not observe the other phases predicted from the structural search.

The organization of this paper is as follows: In Sec. II the computational details and methodology used to perform the calculations are outlined. In Sec. III the Bain and Burgers transformations are applied to austenitic Co_2NiGa and the results are presented. Section IV outlines the minima hopping method as used in this work and the results obtained therein. The phase selection hypothesis is presented and calculations carried out to validate it are discussed in Sec. V. Finally conclusions are drawn in Sec. VI and the work done is summarized.

II. COMPUTATIONAL DETAILS AND METHODOLOGY

The results presented in this work are *ab initio* calculations carried out to determine the electronic, structural, and elastic properties of Co_2NiGa stoichiometric Heusler alloys. The calculations were performed within the framework of density functional theory, as implemented in the Vienna *ab initio* simulation package (VASP) [18], applying the generalized

gradient approximation (GGA) using the Perdew-Wang 1991 (PW91) functional [19]. Single-parameter Burgers path calculations were also carried out using the local density approximation (LDA) [20]. The electronic configurations of the relevant elements were realized using the projector augmented wave (PAW) pseudopotentials formalism [21]. Brillouin zone integrations were performed using a Monkhorst-Pack mesh [22] with at least 5000 k points per Brillouin zone or cell. Full relaxations were realized by using the Methfessel-Paxton smearing method of order 1 [23], and self-consistent static calculations were carried out with the tetrahedron smearing method with Blöchl corrections [24]. A cutoff energy of 350 eV was used for all the Bain and Burgers path calculations and spin polarizations were accounted for as well. Convergence of the electronic structure was assumed, when changes between two consecutive steps fell below 10^{-7} eV.

The elastic constants were calculated by imposing a set of strains $\epsilon = (\epsilon_1,\epsilon_2,\epsilon_3,\epsilon_4,\epsilon_5,\epsilon_6)$ on the crystal structure [25–29]. The stresses (σ_i) resulting from the change in energy due to the deformation are calculated. By application of Hooke's law $\sigma_i = c_{ij}\epsilon_j$, the stiffness tensor c_{ij} may be computed. The bulk modulus (B) is calculated by [29]

$$B = \frac{2}{9}\left(c_{11} + c_{12} + 2c_{13} + \frac{c_{33}}{2}\right). \tag{1}$$

The shear modulus is calculated using the Voigt approximation [29],

$$G = \tfrac{1}{15}(2c_{11} + c_{33} - c_{12} - 2c_{13}+) + \tfrac{1}{5}\left[2c_{44} + \tfrac{1}{2}(c_{11} - c_{12})\right], \tag{2}$$

while Young's modulus is computed by [29]

$$E = \frac{9BG}{3B + G}, \tag{3}$$

and Poisson's ratio may be calculated as

$$\nu = \frac{E}{2G} - 1. \tag{4}$$

III. TRANSFORMATION PATHS IN Co_2NiGa

The crystallographic relations for the bcc-hcp transformation were established by Burgers [13] and can be described as

$$(110)_{bcc} \parallel (0001)_{(hcp)}, \quad [\bar{1}11]_{bcc} \parallel [\bar{2}110]_{hcp}. \tag{5}$$

The transformation manifests in the form of two collective movements of atomic planes: (i) shearing towards the $[\bar{1}11]$ direction along the $(1\bar{1}2)$ plane transforming the (110) bcc plane into the (0001) hcp plane, and (ii) shuffling of alternate (110) planes in the $[0\bar{1}10]$ direction, with a constant (110) interplanar distance. The Burgers mechanism thus involves two distinct and simultaneous structural changes characterized by primary order parameters.

A. 1-parameter Burgers path

Friák *et al.* [30] coupled the two degrees of freedom to obtain a single-parameter Burgers path to study the bcc-hcp transformation in iron [30–32]. This model is modified and applied to the $L2_1 \rightarrow$ hcp transformation in this work. Proceeding in a manner similar to [30], the simplest transformation is accomplished using an orthorhombic basis applied to a $1 \times 2 \times 1$ supercell of a 4-atom unit cell. For a $L2_1$ lattice constant a, the orthorhombic lattice parameters will be

$$a_0 = \frac{\sqrt{2}a}{s(\delta)^{1/3}}, \quad b_0 = a\left(\frac{\delta(2\sqrt{3} - 3\sqrt{2})}{6} + \frac{\sqrt{2}}{2}\right),$$
$$c_0 = a\left(\frac{\delta(2\sqrt{2} - 3)}{3} + 1\right), \tag{6}$$

where

$$s(\delta) = \sqrt{2}\left(\frac{\delta(2\sqrt{3} - 3\sqrt{2})}{6} + \frac{\sqrt{2}}{2}\right)\left(\frac{\delta(2\sqrt{2} - 3)}{3} + 1\right). \tag{7}$$

Here, $\delta = 0$ corresponds to the $L2_1$ phase and $\delta = 1$ represents the hcp phase. Correspondingly, the angle in the (110) $L2_1$ planes evolves from $\theta = 109.47^\circ$ to $\theta = 120^\circ$. The (110) $L2_1$ planes are transformed to the (0001) hcp stacking planes.

In Fig. 1, we present the profile of the differential energy (δE) along the Bain path and single-parameter Burgers paths for CoNiGa. For the Burgers path, $\delta = 1$ corresponds to the perfect hcp lattice type. It is seen that the minimum along the Burgers path occurs at approximately $\delta = 1.1$. The single data point in the figure corresponds to the completely relaxed minimum energy structure. The energy of this structure is noted to be further lowered by about 50 meV upon complete relaxation.

B. 2-parameter Burgers path

When both degrees of freedom are considered, this gives rise to the Burgers surface which determines the energy field for the transformation. Nishitani *et al.* [33] described the bcc-hcp transformation in Ti using the Burgers surface by performing first-principle calculations using a two-parameter model corresponding to the above mentioned two degrees of freedom.

In order to model the Burgers surface of the Co_2NiGa and Co_2NiAl Heusler alloys, keeping the atomic volume constant, the most rigorous transformation path is achieved by using an orthorhombic basis (space group: *CmCm*, No. 59, Pearson symbol: *oS*4) in conjunction with an 8-atom unit cell. The evolution of the basis vectors and atom positions gives rise to a two-dimensional parameter space (δ,η), where δ_1 accounts for the basal shear and η for the shuffle. For a $L2_1$ lattice constant a, the orthorhombic lattice parameters will be

$$a_0 = a\sqrt{2}, \quad b_0 = 2a/s(\delta), \quad c_0 = a\sqrt{2}s(\delta), \tag{8}$$

where

$$s(\delta) = 1 + \left[\left(\frac{3}{2}\right)^{0.25} - 1\right]\delta. \tag{9}$$

The basis vectors are given by $[a_0,0,0]$,$[0,b_0,0]$,$[0,0,c_0]$, with atom positions (0,0.25,0.5), (0,0.75,0), (0.5,0.25,η/6), (0.5,0.75,η/6), (0,0,0), (0.5,0.5,0.5 + η/6), (0,0.5,0), and

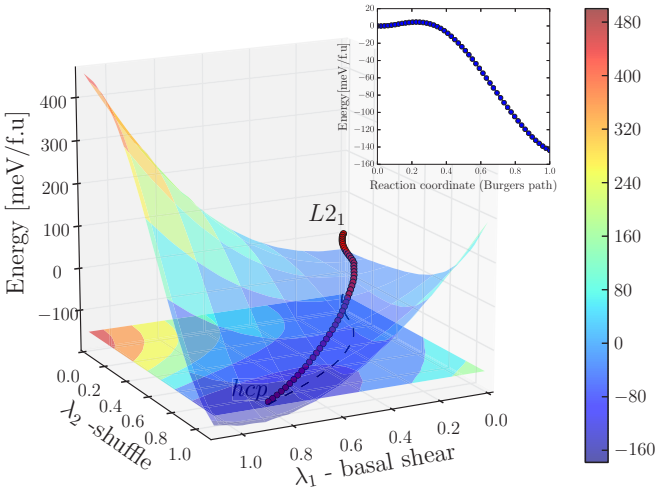

FIG. 2. (Color online) Burgers energy surface for Co_2NiGa Heusler alloys. (0,0) corresponds to the $L2_1$ structure and (1,1) corresponds to the hcp structure. Inset: Energy profile for the transformation.

(0.5,0,0.5 + η/6). The L_21 and hcp phases then correspond to (0,0) and (1,1), respectively.

Figure 2 shows the Burgers energy surface for the Co_2NiGa Heusler alloy considering a two-parameter Burgers path that takes explicit account for shuffles and shears necessary to transform a bcc lattice into an hcp variant. In the figure, (0,0) corresponds to the $L2_1$ structure and (1,1) corresponds to an hcp-like structure.

For these calculations, a 17 × 17 grid was used and the energy of the intermediate structures at each grid point was calculated using methods detailed in Sec. II. A second-order accurate finite difference scheme was then used to compute the total energy surface. The minimum energy path (MEP) for the Burgers transformation through this energy surface was constructed by using the modified string method [34]. This method allows determination of the MEP by finding the minimum energy configuration along the hyperplanes normal to the path. The MEP for the Burgers transformation is also indicated along the surface. The inset shows the energy profile of the transformation, which is again barrierless. The energy values for all the different fully relaxed structures along with their lattice parameters are summarized in Table I.

From Table I, it is seen that both the 1-parameter and 2-parameter Burgers paths yield a stable orthorhombic phase

TABLE I. Lattice parameters and energy values for Co_2NiGa and Co_2NiAl. Calculations were performed using the GGA [19] approximation. Energy difference is computed relative to the $L1_0$ structure in meV/f.u.

Model	Structure	Space Group	a (Å)	b (Å)	c (Å)	δE (meV/f.u.)
	$L2_1$	225	4.015	4.015	4.015	108.402
	$L1_0$	123	4.364	4.364	3.598	0.000
1 parameter	O	59	4.113	5.094	4.397	−68.747
2 parameters			4.484	5.084	4.073	−118.436

appreciably lower in energy than $L1_0$ via barrierless transformations. Subsequently, it was deemed necessary to explore the energy landscape surrounding the $L1_0$ structure by applying the minima hopping methods, the results of which are detailed in the following section.

IV. MINIMA HOPPING METHOD

Minima hopping calculations were carried out for the Co_2-Ni-Ga chemical composition. The basics of the method are described in detail in the original references [14,35]. In summary, this method performs a systematic *ab initio* search for low-enthalpy phases of a given compound, where the only input is the chemical composition and the number of atoms in the simulated cell. Short Rahman-Parrinello molecular dynamics simulations [36] are used to escape from local minima and efficient local geometry relaxations were performed to identify stable configurations. The efficiency of the escape step was ensured by aligning the initial atomic velocities within the molecular dynamics along a soft mode direction. The energy and stresses are obtained by interfacing the method with VASP [18]. As in the total energy calculations, the projector augmented wave (PAW) method was used to describe valence and core electrons [37]. To approximate the exchange-correlation functional we used the Perdew-Burke-Ernzerhof (PBE) [38] generalized gradient approximation. After the potential structures are found by the minima hopping method, the structure is tightly minimized by using a plane wave cutoff of 550 eV, and the k mesh used to calculate the observables in the Brillouin zone is adapted such that the calculation guaranteed a numerical convergence of the total energy to less than 2 meV/atom. The structures were also re-optimized by using other functionals in accordance with the total energy calculations.

A summary of the results is shown in Table II. This table shows the energy of all structures using GGA [19], PBE [38], and LDA [20] approximations relative to the relaxed $L1_0$

TABLE II. Energy difference of the predicted crystal structures in meV/f.u. for Co_2NiGa.

Space Group	δE GGA	PBE	LDA	Structure
123	0	0	0	$L1_0$
3	−58.0920	−21.2160	−67.1520	monoclinic
5	−55.5360	−51.1120	−82.5480	monoclinic
8	−109.976	−100.936	−150.396	monoclinic
11	−139.124	−136.228	−167.192	monoclinic
12	−122.636	−115.444	−159.772	monoclinic
31	−104.456	−99.6720	−136.620	orthorhombic
40	−66.2120	−61.1280	−91.3280	orthorhombic
44	−78.9040	−71.2440	−117.124	orthorhombic
51	−68.9520	−75.6160	−61.2120	orthorhombic
59	−132.536	−144.816	−151.376	O
63	−125.012	−126.512	−152.972	orthorhombic
119	−137.296	−131.360	−183.000	tetragonal
139	−27.9680	−20.7720	−67.9200	tetragonal
216	83.3960	89.4600	94.6720	Inv. Heusler
225	108.402	109.232	78.2080	$L2_1$

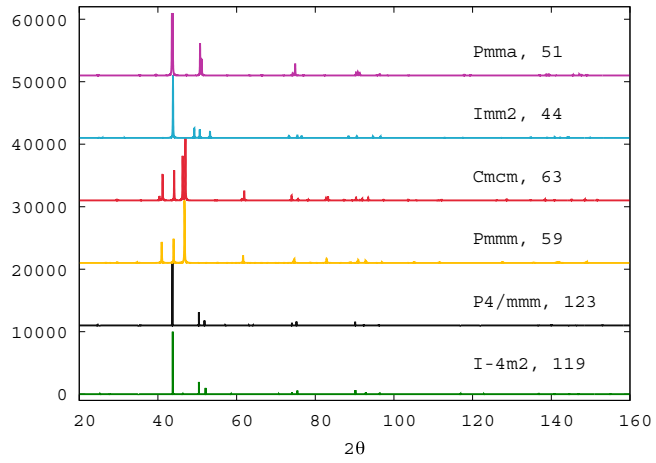

FIG. 3. (Color online) Simulated x-ray diffraction spectrum with Cu Kα radiation, $\lambda = 1.54178$ Å for some of the low-energy structures reported in Table II.

structure. It is seen that a number of structures with monoclinic, tetragonal, and orthorhombic symmetries are predicted with energies much lower than the $L1_0$ structure. The list also includes the O phase, which was observed in Sec. III to result from a Burgers transformation of the original $L2_1$ structure. This shows that a number of low-energy structures theoretically exist in the thermodynamic vicinity of $L1_0$ but have been inaccessible experimentally. Figure 3 shows the simulated x-ray diffraction spectra for some of the lowest-energy structures, that can be used by the experimentalist to compare with some of our low-energy structures. The transformation mechanisms for all these structures, except the O, structure are unknown. The possibility of considering all possible structural transitions from the $L1_0$ phase to the predicted ones is not the focus of this paper. Instead, we focus only on the O structure and conduct a thorough analysis to investigate (i) the stability of the structure and (ii) the possible energy barriers which may render these low-energy structures inaccessible.

V. ANALYSIS AND DISCUSSION

As mentioned earlier, the austenitic phase in the Heusler system Co_2NiGa has a $L2_1$ structure. The martensitic transformation exhibited by this alloy is reversible, giving rise to the shape memory effect. This implies that the resultant martensite has a symmetry which is a subgroup of the austenitic cubic structure [39]. The point group symmetries of the relevant structures are $Fm\bar{3}m$ for $L2_1$, $P4/mmm$ for $L1_0$, and $Pmmn$ for the O phase. The point groups of both the $L1_0$ and the O structures are subgroups of the $L2_1$ point group. The group-subgroup relationship for the (a) $L2_1$-O and (b) $L2_1$-$L1_0$ are shown in Figs. 4(a) and 4(b). Three possible paths exist for the symmetry transformation from $L2_1$ to O while two paths exist for the symmetry transformation from $L2_1$ to $L1_0$. Some examples of group-subgroup relations for additional structures isolated using the minima hopping method, which are close in energy to the O structure, viz., structures corresponding to space groups No. 63 and No. 119, have been described in Figs. 4(c) and 4(d). For both of these structures, we have

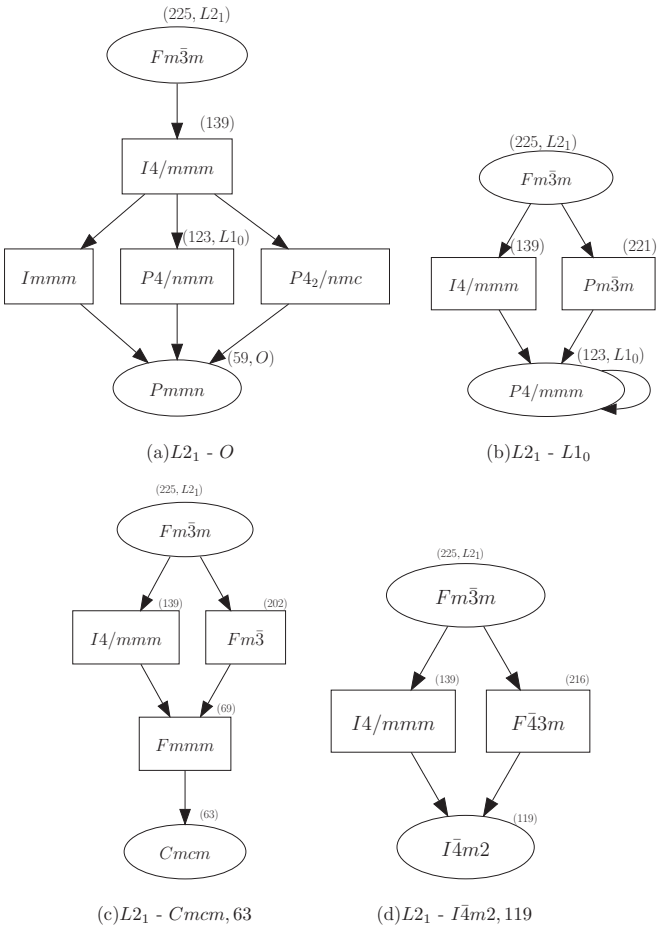

FIG. 4. Group-subgroup graphs for the transformations (a) $L2_1$-O and (b) $L2_1$-$L1_0$ and for space groups (c) 63 and (d) 119 as obtained in Table II generated using the Bilbao crystallographic database. Space groups corresponding to the relevant point groups are indicated.

two possible symmetry-reducing transformations. Of all the structures listed in Table II, structures with space groups 12, 51, 59, 63, 119, 123, and 139 satisfy the symmetry relations with number of symmetry paths ranging between 1 and 5. For space groups 8 and 11, symmetry relations are satisfied, but the number of symmetry paths is 15 and 12, respectively. A larger number of possible symmetry paths amounts to a one to many correspondence, which makes it harder for a material to "remember" its original crystal structure, thereby hindering the ideal shape memory effect. The remaining structures (space groups 3, 5, 31, 40, 44) do not satisfy the symmetry requirements. Thus, from a crystallographic point of view, it is seen that in addition to the O phase,a number of other structures also satisfy requirements.

The ideal reversible martensitic transformation must also be a volume-preserving transition [39] since the higher the volume change, the greater is the hysteresis or irreversibility associated with the transformation. Having established the fact that there is a group-subgroup relation between $L2_1$ and the O phase, we proceeded to investigate the existence of possible barriers to the transformation. Table III shows the volume change (δV) associated with the $L2_1$-O and

TABLE III. Energy difference due to volume changes during transformation. Indicated are the volume change (δV) for the transformations, the effective bulk modulus for the transformation (B_e), the corresponding volumetric strain energy per unit volume (E_v), and the total energy for the transformation (E_t).

Transformation	δV (Å^3)	B_e (GPa)	E_v (meV/f.u.)	E_t (meV/f.u.)
$L2_1$-O	−0.28	145	−0.784	−226.838
$L2_1$-$L1_0$	−0.12	142.5	−0.141	−108.402

$L2_1$-$L1_0$ transformations, the effective bulk modulus for the transformation (B_e), the corresponding volumetric strain energy per unit volume (E_v), and the total energy for the transformation (E_t). The volumetric strain energy was calculated as

$$E_v = \tfrac{1}{2}\sigma_v\epsilon_v = \tfrac{1}{2}(B_e\epsilon_v)\epsilon_v = \tfrac{1}{2}B_e{\epsilon_v}^2, \qquad (10)$$

where σ_v is the volumetric stress and ϵ_v is the volumetric strain. ϵ_v was calculated by taking the ratio of change in volume (δV) to original volume. B_e was estimated by averaging the bulk moduli for the austenitic and martensitic phases. In Table III, it is apparent that the volumetric strain energy associated with the $L2_1$-O is about 5 times larger than that for the $L2_1$-$L1_0$ transformation; however when compared to the E_t, it it seen that its contribution is negligible. Also, one must keep in mind that bulk effects (such as those associated with elastic strain energy) only become important as the system volume becomes large enough. The possible nucleation of the O phase from a parent $L2_1$ matrix is thus not ruled out.

A. The phase selection problem

Recapitulating, the Co_2NiGa Heusler alloy shows a phase transformation from the austenitic, high-temperature $L2_1$ structure to the martensitic, low-temperature nonmodulated $L1_0$ phase. Minima hopping calculations predict a number of structures with monoclinic, tetragonal, and orthorhombic symmetries with energies much lower than the $L1_0$ structure. Furthermore, Burgers path calculations predict the existence of a martensitic phase with orthorhombic symmetry, the O phase. This phase is stable against perturbations along a Burgers transformation in a barrierless fashion. While the examination of possible elastic energy barriers to the transformation suggested that there may be some elastic constraints to the stabilization of the O phase, the elastic energy may not be sufficient to completely rule it out.

It is proposed that the absence of the O phase may be attributed to the problem of phase selection. As seen in Fig. 5, a possibility exists that while the O phase is relatively more stable than the $L1_0$ phase, the energy barrier for the $L2_1$-O transformation may be higher than the barrier to the $L2_1$-$L1_0$ transformation, i.e., $\delta E_b > \delta E_g$ at some temperature far away from the ground state conditions, when the system is cooled from the $L2_1$ structure. In this case, the high-temperature austenitic phase may not be able to sample a subset of low-energy states since there may be no accessible paths. We proceeded to examine the stability of the O phase in terms of its vibrational spectrum and its elastic constant tensor, and we also examined the effect of configurational and magnetic disorder (brought about by high temperatures) on the competition between Bain and Burgers paths, taking the $L2_1$ structure into either the observed $L1_0$ or the missing O phase.

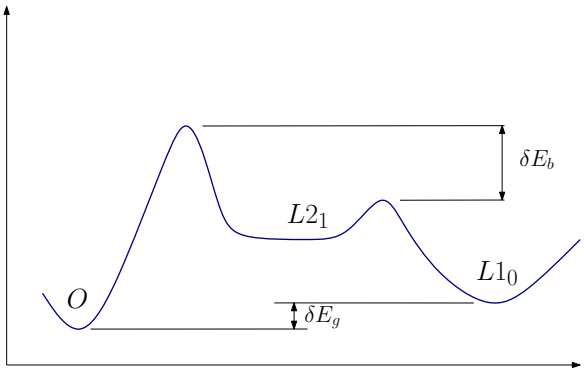

FIG. 5. (Color online) Schematic of relative stabilities of the $L1_0$ and the O structures in the Co-Ni-Ga heusler alloy. δE_g is the energy difference between the conventional martensitic phase $L1_0$ and the O phase. δE_b is the proposed difference between the energy barriers for the $L2_1$-O transformation and the $L2_1$-$L1_0$ transformation.

B. Phase stability analysis

1. *Vibrational properties*

Phonon calculations were carried out to study the relative stability of the $L2_1$, $L1_0$, and O structures. We used the FITFC module as implemented in the ATAT package to perform the vibrational calculations. This method consists of slightly perturbing the positions of the atoms away from their equilibrium position and calculating the reaction forces by fitting a spring model. Equating the calculated forces to the forces predicted from the harmonic model yields a set of linear constraints that allows the unknown force constants to be determined. The force constant matrix is then used to extract the projected vibrational density of states and the phonon dispersion curves. The projected vibrational density of states is shown in Fig. 6.

The mode of interest in these alloys is along the [110] direction. The calculated phonon dispersion curves of the three structures were compared. Figure 7 shows the projected vibrational density of states for these structures along the [ξ,ξ,0] directions in the Co_2NiGa systems. No unstable modes are observed. Softening of the optical modes is observed in the $L1_0$ as well as the O structures. No conclusions can be drawn about the relative stability of the structures. The vibrational contribution to the total energy was estimated for the three structures by integrating over the vibrational density of states. However, the contributions were negligible (<5 meV); hence we do not include them in this work.

2. *Elastic properties*

Elastic constants for the structures considered in this work were calculated as explained in Sec. II and are listed in Table IV in GPa. Included are the significant components of the stiffness tensor (c_{11}, c_{12}, c_{13}, c_{33}, and c_{44}), bulk modulus (B), shear modulus (G), elastic modulus (E), and Poisson's

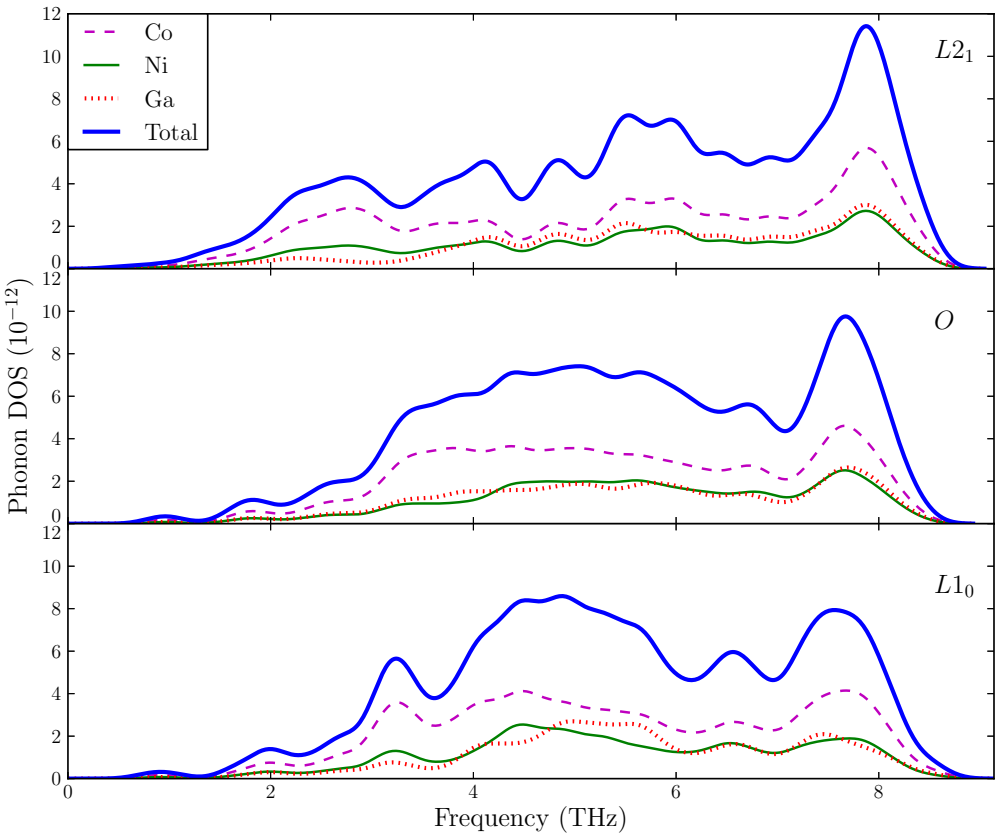

FIG. 6. (Color online) Projected vibrational density of states for the Co_2NiGa system at $T = 0$ K.

ratio (ν). From the table we see that the elastic moduli of $L1_0$ and O structures are close in magnitude. There is no suggestion of instability. $c_{11} - c_{12}$ lends an insight into the stability of the structure with respect to shear and other martensitic transformation inducing deformations. For the $L2_1$ structure, $c_{11} - c_{12} < 0$, which is expected since the $L2_1$

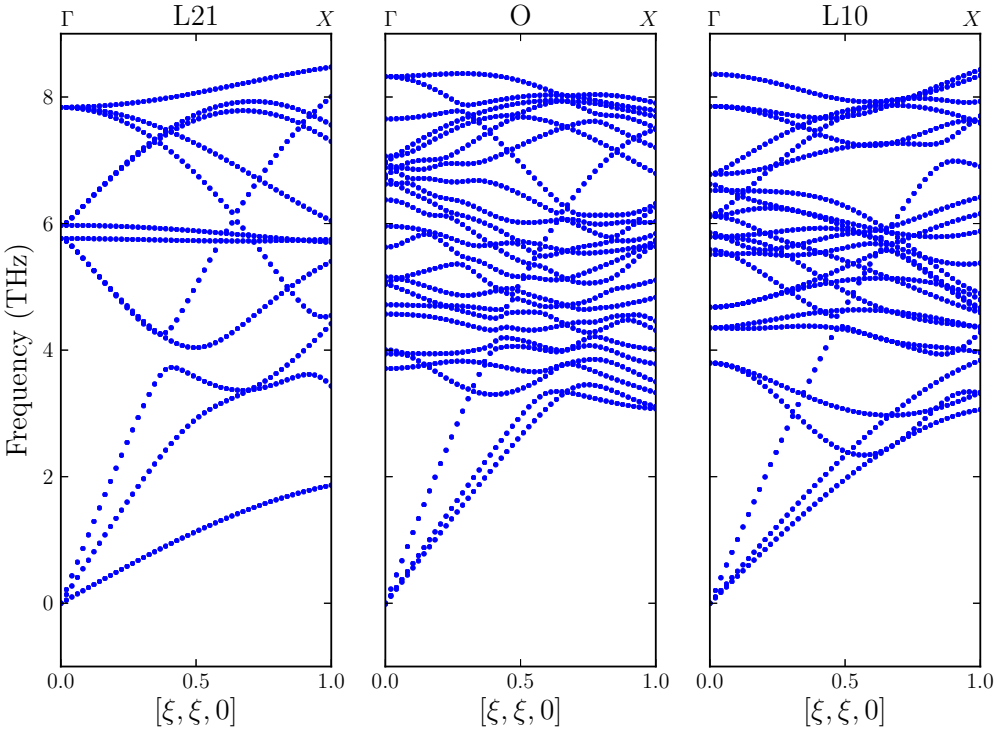

FIG. 7. (Color online) Phonon dispersion curves along the $[\xi,\xi,0]$ direction for the Co_2NiGa system at $T = 0$ K.

TABLE IV. Calculated elastic properties of CoNiGa in GPa: significant components of the stiffness tensor (c_{ij}), bulk modulus (B), shear modulus (G), elastic modulus (E), and Poisson's ratio (ν). Calculations were performed using the GGA [19] approximation.

Alloy	Structure	c_{11}	c_{12}	c_{13}	c_{33}	c_{44}	B	G	E	ν
CoNiGa	$L2_1$	181	186	186	181	141	136	52	139	0.33
	$L1_0$	252	153	163	204	114	149	71	184	0.29
	O	265	154	108	328	55	154	66	173	0.31

structure is unstable with respect to temperature and undergoes a martensitic transformation. However $c_{11} - c_{12}$ values for both $L1_0$ and O structures are positive, with the value for the O phase being higher indicating increased stability with respect to the $L1_0$ structure.

C. Effect of disorder on the competition between Bain and Burgers paths

While arguments using rough estimates for the elastic strain energy associated with the $L2_1$-$L1_0$ and $L2_1$-O transformations suggest a higher elastic barrier for the latter, these arguments cannot be used when looking at the incipient process of the formation of a new phase out of the $L2_1$ matrix since at early stages of the phase transformation bulk energy contributions may not be significant enough. On the other hand, the phonon and elastic calculations suggest that the O phase is mechanically stable. This leads us to believe that there exist mechanisms arising from hitherto unaccounted for contributions within the material which make these low-energy states inaccessible when coming from high-temperature experiments. We thus proceed to examine three such contributions: (i) the effect of configurational disorder, (ii) magnetic disorder, and (iii) atomic disorder.

1. Effect of configurational disorder

It is well known that atomic ordering may influence the transformation behavior of SMAs. Substantial experimental and numerical work has been carried out in investigating the order-disorder transition, long-range ordering, and effect of ordering on the phase transformation characteristics in various shape memory alloys [40–42]. Recarte *et al.* show that in Ni-Mn-In SMA, the thermodynamics of the martensitic transformation depends on the atomic ordering [42]. The effect of configurational disorder was simulated by using special quasirandom structures (SQS) [43], implemented using the ATAT toolkit. A 32-atom supercell was used and the Bain and Burgers paths were recalculated for this structure and are shown in Fig. 8. We see that the energy at the minimum along the Bain path is still higher than that along the Burgers path, although the energy difference is substantially lowered (≈25 meV).

2. Effect of magnetic disorder

In this subsection, we present Bain path and Burgers path calculations for varying degrees of magnetization (100%–0%). This may be viewed as a crude method to simulate the effect of high temperatures by lowering the magnetization.

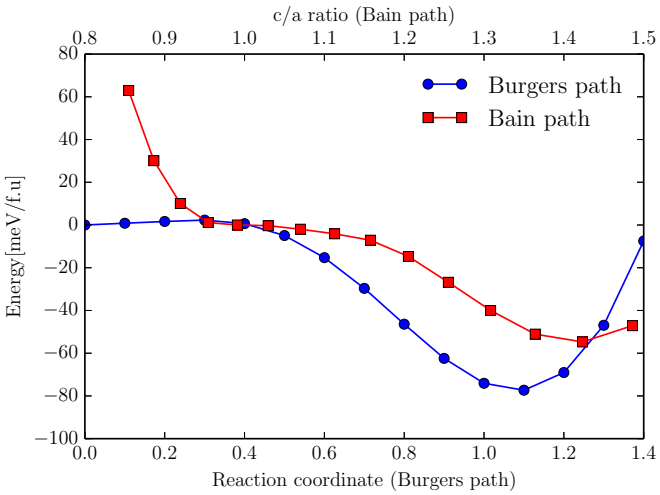

FIG. 8. (Color online) Energy profile comparison for Bain and single-parameter Burger paths in disordered (SQS) Co_2NiGa.

This is achieved by using the fixed spin moments method within VASP. Specifically, we assign a value to the parameter NUPDOWN in the INCAR file. Fixing the value of this parameter ensures that the difference of the number of electrons in the up and down spin component will be kept fixed to the specified value. We calculate the Bain and Burgers paths for the different values of NUPDOWN. For these calculations, VASP automatically sets MAGMOM = NUPDOWN/number of ions; hence we use the term MAGMOM to denote the different cases. Results are presented for 100%, 90%, 70%, 50%, 30% magnetic moment values and the nonmagnetic case.

In Fig. 9, it is seen that for the 100% MAGMOM case, as seen before, the Burgers path has a lower minima than the Bain path; i.e., the O phase is more stable than the $L1_0$ phase. However, on lowering the magnetic moment, as in Fig. 9(b), the Burgers and Bain paths have almost coinciding minima. On further lowering the magnetic moment as in Figs. 9(c)–9(f), the trend is reversed and the Bain path is seen to have an increasingly lower minima than the Burgers path. Thus reducing the magnetization of the system, i.e., introducing magnetic disorder and simulating the effect of higher temperatures, stabilizes the $L1_0$ phase with respect to the O phase.

3. Effect of nonstoichiometric composition

In this section we account for the effect of atomic disorder, viz., the modeling of the transformation in a nonstoichiometric composition. As observed in [1], it is not simple to achieve the perfect Heusler composition Co_2NiGa because one is very near the two-phase ($\gamma + \beta$) region or at the border of the $B2$ phase. Simulating a nonstoichiometric composition also weakens the magnetic ordering naturally (as opposed to fixed-spin calculations in Sec. V C 2). We use a 16-atom SQS supercell to model the the $Co_{43.75}Ni_{25}Ga_{31.25}$ composition and calculate the Bain path. Since the symmetry of the structure is lowered due to the off-stoichiometric composition, the Bain path (varying of c/a) was calculated for 2 cases: (i) $c||z$ and (ii) $c||y$. We then selected the Bain path with the lower

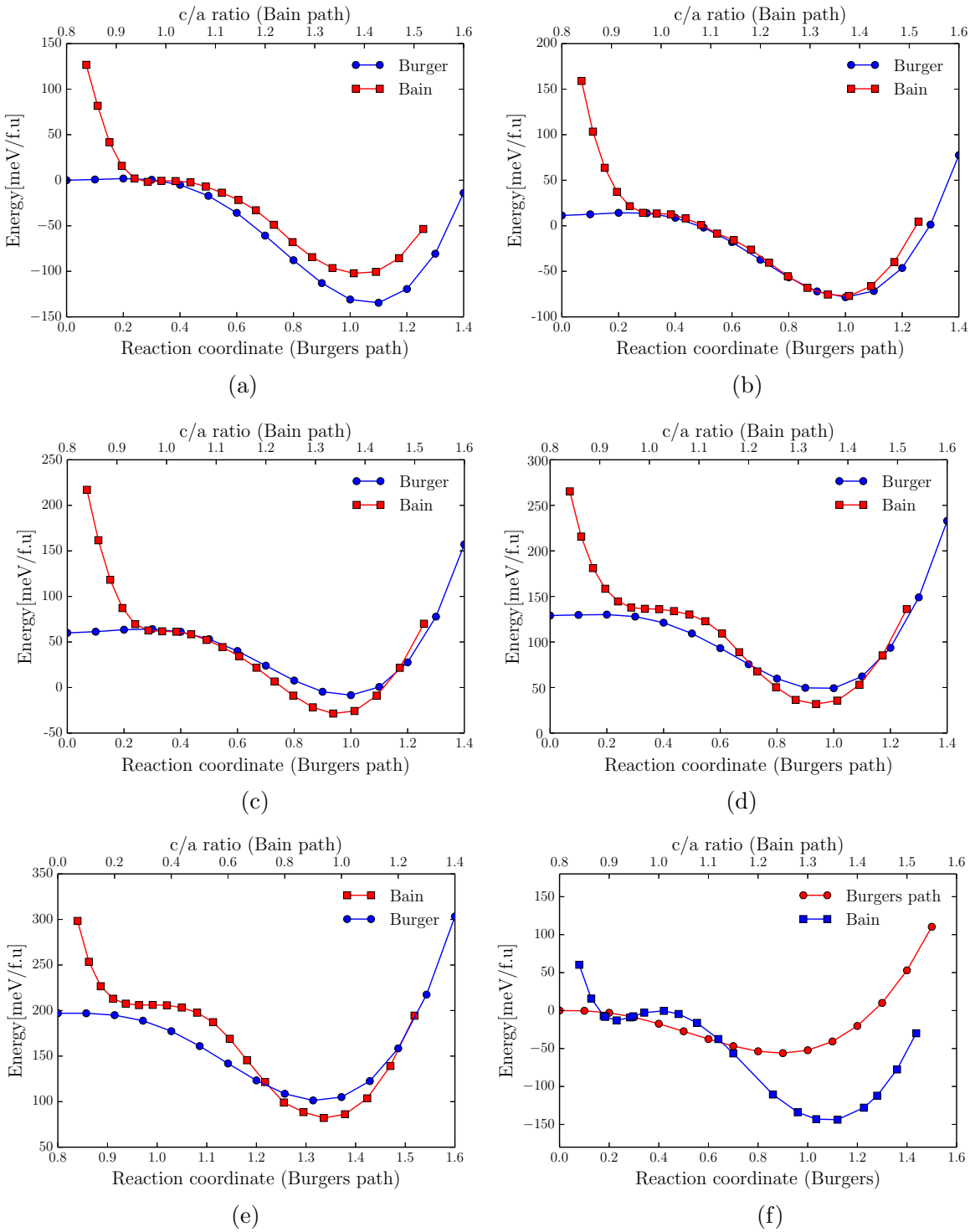

FIG. 9. (Color online) Energy profile comparison for Bain and single-parameter Burgers paths in Co_2NiGa for varying values of magnetization (fixed spin moment calculations): (a) MAGMOM = 100%, (b) MAGMOM = 90%, (c) MAGMOM = 70%, (d) MAGMOM = 50%, (e) MAGMOM = 30%, (f) nonmagnetic.

energy profile. For the Burgers path, we used a simple 16-atom supercell to simulate the structure. Since Ga replaces Co, we considered all possible configurations of Ga replacing Co and then selected the lowest-energy configuration. The Burgers path was carried out on the lowest-energy configuration. Thus it was ensured that the lowest possible Bain path and Burgers paths were used, which encapsulate all possible energy ranges which may be observed and enable us to make a qualitative, if not quantitative, observation. The results are indicated in Fig. 10. It is seen that the $L1_0$ structure as achieved through the Bain path is more stable than the corresponding O phase for this composition. This may be attributed to the weakening of the magnetic ordering due to substitution of one Co atom by a Ga atom, as mentioned earlier.

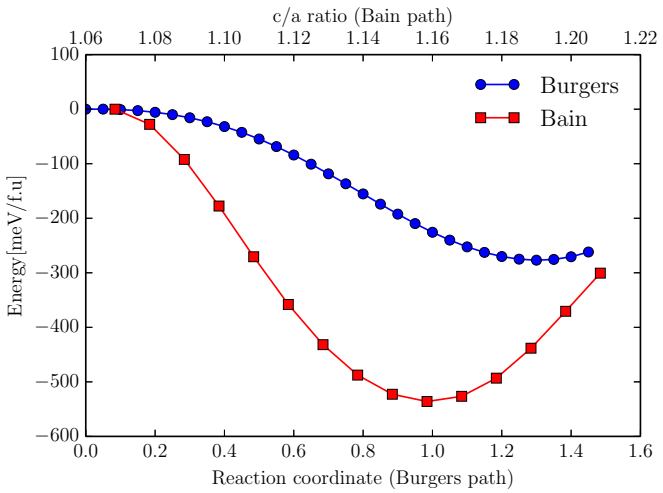

FIG. 10. (Color online) Energy profile comparison for Bain and single-parameter Burgers paths in $Co_7Ni_4Ga_5$.

VI. SUMMARY AND CONCLUSION

The Burgers path was investigated in the Co-Ni-Ga ferromagnetic shape memory alloy system. Calculations were carried out using two models: a single-parameter characterization of the Burgers path and a two-parameter Burgers model which generates a transformation energy surface. In both models, a low-energy structure with an orthorhombic symmetry (O) is observed whose parameters are shifted from the expected coordinates for the transformation. This low-energy structure (O) has been unobserved experimentally. Complete relaxation of the O structure shows further reduction in energy. The Bain path for the alloys is also determined and compared to the Burgers path. Minima hopping calculations were carried out to investigate the energy landscapes surrounding the $L1_0$ martensitic phase in Co-Ni-Ga. Results showed the existence of a number of structures similar in energy to as well as much lower than the predicted O phase in the vicinity of the $L1_0$ structure. It was postulated the the Co_2NiGa Heusler system exhibits a classic case of the phase selection problem. Although the unexpected O phase may be relatively more stable than the $L1_0$ phase, the energy barrier for the $L2_1$-O transformation may be much higher than the barrier to the $L2_1$-$L1_0$ transformation. This high barrier may be due to vibrational effects, elastic effects, configurational disorder, magnetic disorder, or microstructural effects.

In an effort to validate this hypothesis, the stability of this structure was investigated via elastic and lattice dynamics calculations and the contributions of configurational and magnetic disorder on the transformations were studied. No instabilities due to vibrational effects were detected. Elastic calculations showed comparable values of elastic properties for the $L1_0$ and O phases. $c_{11} - c_{12}$ values showed that the O phase is relatively more stable than the $L1_0$ phase. Calculations incorporating configurational disorder showed a lowering in the energy difference between the $L1_0$ and the O structures, but the O structure was still more stable. The calculations simulating the effect of magnetic disorder/high temperature showed that the $L1_0$ structure may be stabilized with respect to the O phase by lowering the magnetic moment. Thus, it is proposed that magnetic disorder plays an important role in the phase selection energetics of the CoNiGa system and is a principal contributor in the determination of the transformation path followed in this system. Further calculations were carried out on an off-stoichiometric composition $Co_{43.75}Ni_{25}Ga_{31.25}$, where the weakening of the magnetic ordering manifests naturally. As expected, the $L1_0$ phase was seen to be more stable than the O phase.

Reverting to the question raised in Sec. I, we conclude that it is unrealistic to use standard DFT prototypes to investigate ground states of relatively less known systems. By performing a detailed analysis of the transformation paths (Burgers and Bain) by taking into account perturbations on the ground state, it is seen that what is manifested is in principle a phase selection problem: the ultimate crystal structure that the system transforms into depends on the path that the system prefers. When coming from high temperature, the accessible path is that corresponding to the Bain transformation. To conclude, discrepancies between DFT and experiments may be reconciled if we consider the "history" of the alloy.

ACKNOWLEDGMENTS

R.A. and A.T. acknowledge support from NSF through Grants No. CMMI-0953984, No. DMR-0805293, and No. DMR-DMR-0844082 [International Institute for Multifunctional Materials for Energy Conversion (IIMEC)[. First-principles calculations by R.A. and A.T. were carried out in the Chemical Engineering Cluster and the Texas A&M Supercomputing Facility at Texas A&M University as well as the Texas Advanced Computing Center (TACC) at the University of Texas at Austin. Preparation of the input files and analysis of the data have been performed within the framework of AFLOW/ACONVASP developed by Stefano Curtarolo as well as with the ATAT package developed by Axel van de Walle. A.T. would like to acknowledge the contribution of Mario Siewart towards preliminary calculations. We also acknowledge the support from the Extreme Science and Engineering Discovery Environment (XSEDE), which is supported by National Science Foundation Grant No. ACI-1053575. P.E. acknowledges support by Deutsche Forschungsgemeinschaft (Priority Programme SPP 1599). A.H.R. and I.V.-J. acknowledge support from CONACYT under Project No. 152153. A.H.R. also acknowledges the support of NSF through DMREF-NSF 1434897 and the donors of the American Chemical Society Petroleum Research Fund for partial support of this research under Contract No. 54075-ND10. We are thankful to M. Amsler and S. Goedecker for useful discussions and the use of their minima hopping implementation. FQ

[1] M. Siewert, M. E. Gruner, A. Dannenberg, A. Hucht, S. M. Shapiro, G. Xu, D. L. Schlagel, T. A. Lograsso, and P. Entel, Phys. Rev. B **82**, 064420 (2010).

[2] X. Dai, G. D. Liu, Z. H. Liu, G. H. Wu, J. L. Chen, F. B. Meng, H. Y. Liu, L. Q. Yan, J. P. Qu, Y. X. Li *et al.*, Appl. Phys. Lett. **87**, 112504 (2005).

[3] J. Liu, M. Xia, Y. Huang, H. Zheng, and J. Li, J. Alloys Compd. **417**, 96 (2006).
[4] E. Dogan, I. Karaman, Y. I. Chumlyakov, and Z. P. Luo, Acta Mater. **59**, 1168 (2011).
[5] D. Canadinc, J. Dadda, H. J. Maier, I. Karaman, H. E. Karaca, and Y. I. Chumlyakov, Smart Mater. Struct. **16**, 1006 (2007).
[6] K. Oikawa, L. Wulff, T. Iijima, F. Gejima, T. Ohmori, A. Fujita, K. Fukamichi, R. Kainuma, and K. Ishida, Appl. Phys. Lett. **79**, 3290 (2001).
[7] Y. Murakami, D. Shindo, K. Oikawa, R. Kainuma, and K. Ishida, Acta Mater. **50**, 2173 (2002).
[8] A. Dannenberg, Ph.D. thesis, Universität Duisburg-Essen, Fakultät für Physik Theoretische Physik, 2011.
[9] T. Yamada, T. Ikeda, R. P. Stoffel, V. L. Deringer, R. Dronskowski, and H. Yamane, Inorg. Chem. **53**, 5253 (2014).
[10] J. Liu, H. Xie, Y. Huo, H. Zheng, and J. Li, J. Alloys Compd. **420**, 145 (2006).
[11] T. Fichtner, C. Wang, A. A. Levin, G. Kreiner, C. S. Mejia, S. Fabbrici, F. Albertini, and C. Felser, Metals **5**, 484 (2015).
[12] P. Tolédano and V. Dmitriev, *Reconstructive Phase Transitions* (World Scientific, 1996).
[13] W. G. Burgers, Physica **1**, 561 (1934).
[14] S. Goedecker, J. Chem. Phys. **120**, 9911 (2004).
[15] A. Jain, S. P. Ong, G. Hautier, W. Chen, W. D. Richards, S. Dacek, S. Cholia, D. Gunter, D. Skinner, G. Ceder, and K. A. Persson, APL Mater. **1**, 011002 (2013).
[16] J. Saal, S. Kirklin, M. Aykol, B. Meredig, and C. Wolverton, JOM **65**, 1501 (2013).
[17] S. Curtarolo, G. Hart, W. Setyawan, M. Mehl, M. Jahnatek, R. Chepulskii, O. Levy, and D. Morgan, AFLOW: Software for high-throughput calculation of material properties, 2009.
[18] G. Kresse and J. Furthmüller, Phys. Rev. B **54**, 11169 (1996).
[19] J. P. Perdew and Y. Wang, Phys. Rev. B **45**, 13244 (1992).
[20] J. P. Perdew and A. Zunger, Phys. Rev. B **23**, 5048 (1981).
[21] P. E. Blöchl, Phys. Rev. B **50**, 17953 (1994).
[22] H. Monkhorst and J. Pack, Phys. Rev. B **13**, 5188 (1976).
[23] M. Methfessel and A. T. Paxton, Phys. Rev. B **40**, 3616 (1989).
[24] P. E. Blöchl, O. Jepsen, and O. K. Andersen, Phys. Rev. B **49**, 16223 (1994).
[25] S. Ganeshan, S. Shang, Y. Wang, and Z.-K. Liu, Acta Mater. **57**, 3876 (2009).
[26] S. Ganeshan, S. Shang, H. Zhang, Y. Wang, M. Mantina, and Z. Liu, Intermetallics **17**, 313 (2009).
[27] S. Shang, A. Saengdeejing, Z. Mei, D. Kim, H. Zhang, S. Ganeshan, Y. Wang, and Z. Liu, Comput. Mater. Sci. **48**, 813 (2010).
[28] Y. Le Page and P. Saxe, Phys. Rev. B **65**, 104104 (2002).
[29] T. Duong, S. Gibbons, R. Kinra, and R. Arróyave, J. Appl. Phys. **110**, 093504 (2011).
[30] M. Friák and M. Šob, Phys. Rev. B **77**, 174117 (2008).
[31] M. Šob, M. Friák, L. Wang, and V. Vitek, in *MRS Proceedings*, Vol. 538 (Cambridge University Press, 1998).
[32] M. Šob, M. Friák, L. Wang, and V. Vitek, (1999).
[33] S. Nishitani, H. Kawabe, and M. Aoki, Mater. Sci. Eng., A **312**, 77 (2001).
[34] A. Samanta *et al.*, arXiv:1009.5612.
[35] M. Amsler and S. Goedecker, J. Chem. Phys. **133**, 224104 (2010).
[36] M. Parrinello and A. Rahman, J. Appl. Phys. **52**, 7182 (1981).
[37] P. E. Blöchl, Phys. Rev. B **50**, 17953 (1994).
[38] J. P. Perdew, K. Burke, and M. Ernzerhof, Phys. Rev. Lett. **77**, 3865 (1996).
[39] K. Bhattacharya, available from bhatta@co.caltech.edu.
[40] N. Singh, E. Dogan, I. Karaman, and R. Arróyave, Phys. Rev. B **84**, 184201 (2011).
[41] E. Obradó, L. Mañosa, and A. Planes, Phys. Rev. B **56**, 20 (1997).
[42] V. Recarte, J. I. Pérez-Landazábal, V. Sánchez-Alarcos, and J. A. Rodríguez-Velamazán, Acta Mater. **60**, 1937 (2012).
[43] A. Zunger, S.-H. Wei, L. G. Ferreira, and J. E. Bernard, Phys. Rev. Lett. **65**, 353 (1990).